NeuroImage 221 (2020) 117153

Contents lists available at ScienceDirect

NeuroImage

journal homepage: www.elsevier.com/locate/neuroimage

Identification of competing neural mechanisms underlying positive and negative perceptual hysteresis in the human visual system

Alexandre Sayal [a,b,e,1], Teresa Sousa [a,b,1], João V. Duarte [a,b], Gabriel N. Costa [a,b], Ricardo Martins [a,b], Miguel Castelo-Branco [a,b,c,d,*]

[a] Coimbra Institute for Biomedical Imaging and Translational Research (CIBIT), University of Coimbra, Portugal
[b] Institute of Nuclear Sciences Applied to Health (ICNAS), University of Coimbra, Portugal
[c] Faculty of Medicine, University of Coimbra, Portugal
[d] ICNAS Produção, University of Coimbra, Portugal
[e] Siemens Healthineers, Portugal

ARTICLE INFO

Keywords:
Perceptual decision
Hysteresis
Perceptual history
Bistable visual motion

ABSTRACT

Hysteresis is a well-known phenomenon in physics that relates changes in a system with its prior history. It is also part of human visual experience (perceptual hysteresis), and two different neural mechanisms might explain it: persistence (a cause of positive hysteresis), which forces to keep a current percept for longer, and adaptation (a cause of negative hysteresis), which in turn favors the switch to a competing percept early on. In this study, we explore the neural correlates underlying these mechanisms and the hypothesis of their competitive balance, by combining behavioral assessment with fMRI. We used machine learning on the behavioral data to distinguish between positive and negative hysteresis, and discovered a neural correlate of persistence at a core region of the ventral attention network, the anterior insula. Our results add to the understanding of perceptual multistability and reveal a possible mechanistic explanation for the regulation of different forms of perceptual hysteresis.

1. Introduction

The response of non-linear dynamic systems may depend not only on the current input but also on their history. When the transition between two states of a system is affected by recent history, we observe hysteresis (Mayergoyz, 2003). The concept arose originally from physical sciences but has raised interest among researchers in other fields, such as electronics (Mandal et al., 2014; Torre and Masoller, 2010), cardiology (Lorent and Davidenko, 1990; Zaniboni, 2018) and cognitive neuroscience (Kleinschmidt et al., 2002; Pisarchik et al., 2014; Williams et al., 1986; Wilson, 1977).

Perceptual hysteresis reflects not only the fact that perceptual stability thresholds depend on the context, but also on the effects of the previous perceptual experience, carrying the recent history of a percept into the present (Frackowiak et al., 2004). In the field of visual perception, it has been explored in a number of behavioral studies with paradigms of letter recognition (Kleinschmidt et al., 2002), binocular rivalry (Buckthought et al., 2008; Wilson, 1977), apparent motion (Hock et al., 1993), motion direction detection (Williams et al., 1986), and emotion recognition (Sacharin et al., 2012; Liaci et al., 2018).

Classically, hysteresis has been linked to a mechanism of lag or persistence of a state, despite input parameter changes to values favoring the alternative one. In other words, the transition to the opposing percept occurs later than in a control situation (where there is no influence of recent history). However, it has become necessary to refer to this phenomenon as positive hysteresis, given evidence for the inverse phenomenon - negative hysteresis: the transition to the opposing percept occurs sooner than the control condition, revealing a link to a mechanism of habituation or adaptation (Assad et al., 1989; Lorent and Davidenko, 1990; Babu and Wanare, 2011; Laval, 2011; Mandal et al., 2014; Pisarchik et al., 2014; Liaci et al., 2018; Schwiedrzik et al., 2014; Torre and Masoller, 2010; Lopresti-Goodman et al., 2013).

In the domain of motion perception, (Williams et al., 1986) found that when perception alternated between seeing completely random motion and upward coherent flow, the switch point depended on the recent perceptual history. This behavioral result was identified by the authors as hysteresis in the perception of motion direction and was interpreted as resulting from cooperative interactions between neurons with similar

* Corresponding author. ICNAS - Institute of Nuclear Sciences Applied to Health, University of Coimbra Polo 3, 3000-548, Coimbra, Portugal.
E-mail address: mcbranco@fmed.uc.pt (M. Castelo-Branco).
[1] Both authors contributed equally.

https://doi.org/10.1016/j.neuroimage.2020.117153
Received 15 February 2020; Received in revised form 2 July 2020; Accepted 6 July 2020
Available online 11 July 2020

directional tuning and inhibitory interactions between neurons with different tuning. Afterward, in a number of studies using apparent motion, Hock and colleagues (Hock and Schöner, 2010; Hock et al., 1997; Hock et al., 1993) have demonstrated that even when controlling for certain factors such as anticipation, inferences about task structure, or response perseverance, perceptual hysteresis is still found. This raises the need to identify the underlying neural correlates of this phenomenon. Perceptual hysteresis might provide a powerful tool to understand our perceptual representations and how competition between decision mechanisms evolve as a function of previous experience, which is particularly relevant for the understanding of perceptual stability.

Perceptual stability is usually studied under conditions of multistability, where multiple perceptual solutions are possible under the same sensory input. In the motion domain, this is related to the aperture problem: when a moving straight line is viewed through an aperture so that its endpoints are not visible, only the component of the motion perpendicular to the line orientation is perceived (Wallach, 1935; Wuerger et al., 1996). The resolution of the ambiguity inherent to this problem requires the understanding of the mechanisms responsible for computing a global percept from many isolated local cues. Even though there are many published studies exploring these mechanisms (Anstis and Kim, 2011; Castelo-Branco et al., 2002; Huguet et al., 2014; Wang et al., 2013; Sousa et al., 2018; Duarte et al., 2017), it is still not clear what is the influence of perceptual history on perceptual switches during continuous stimulus observation (Pearson and Brascamp, 2008; Sterzer et al., 2009; Brascamp et al., 2018). A classic example of an ambiguous visual stimulus, resulting from the aperture problem, is when two moving gratings are superimposed to become a plaid (Adelson and Movshon, 1982; Wallach, 1935). The perception of the plaid stimulus switches back and forth between two interpretations: it can be perceived either as a single surface moving rigidly (coherent motion) or as two surfaces sliding over each other (incoherent motion).

Here, we aimed to investigate the neural mechanisms underlying hysteresis during the continuous interpretation of a moving plaid. We hypothesize two mechanisms of perceptual history: one which forces the perceptual switch sooner than the control, and other which delays the perceptual switch (Lopresti-Goodman et al., 2013; Schwiedrzik et al., 2014; Fritsche et al., 2017; Liaci et al., 2018). The interaction between these two mechanisms can result in one of four effects: positive hysteresis (the current percept is kept for longer), negative hysteresis (early switch to the alternative percept), null or undefined. Moreover, we hypothesize that we can only infer the neural mechanism behind perceptual hysteresis when comparing with a non-history case.

Recently, it was shown that previous experience could induce opposite biases in perception and decision (Fritsche et al., 2017), further emphasizing the need to elucidate the neural mechanisms that underlie these perceptual biases. In an independent study, we have shown that adaptation can contribute to regulating percept duration during visual bistability, with distinct weights, depending on the type of percept (Sousa et al., 2018). In the current study, we aimed to understand how such adaptation competes with persistence to influence perceptual experience, and the neural correlates underlying hysteresis. There is an ongoing debate on this issue, with some authors providing models that try to explain persistence and adaptation with a single mechanism (Gepshtein and Kubovy, 2005), while others suggest the opposite (Wilson, 2017; Wilson, 2007). Importantly, a recent neurophysiological study has shown that persistence and adaptation map into distinct neural networks (Schwiedrzik et al., 2014), probably ascribed to interactions between early and higher-order processing stages, as postulated previously by some authors (Gigante et al., 2009; Sterzer and Rees, 2008). Our competition hypothesis, here added to the debate, arises from previous evidence of lower positive hysteresis for longer adaptation periods (Buckthought et al., 2008) and of altered brain activity due to hysteresis in adaptation responsive regions (Kleinschmidt et al., 2002).

This behavioral and neuroimaging study also allowed us to test the contribution of high and low-level mechanisms to visual motion bistability. It follows the hypothesis that perceptual persistence depends on high-level neural mechanisms, while adaptation arises from more automatic and low-level mechanisms (Schwiedrzik et al., 2014; Kleinschmidt et al., 2002). Concerning low-level regions, we focused on the human motion complex (hMT+), the key visual area involved in motion perceptual decision, which plays a major role in neural adaptation (Huk and Heeger, 2002; Sousa et al., 2018), while also investigating the role of other brain regions involved in global motion perception. Concerning high-level regions, we focused on the anterior insula. It has been widely shown that this region is involved in perceptual decision-making, ambiguous choice, and evidence accumulation (Rebola et al., 2012; Lamichhane et al., 2016; Duarte et al., 2017). Such a critical role is consistent with the notion that it contributes to the choice of relevant perceptual content, as a core of salience and ventral attentional networks (Corbetta and Shulman, 2002; Uddin, 2014). Interestingly, its role in perception-driven processing within the ventral attentional network has been suggested to be right-lateralized, unlike its role within the salience network (Eckert et al. 2009; Uddin 2014; Zhang et al. 2018). However, lateralization effects remain controversial.

Our results show evidence for a continuous competition between perceptual history mechanisms. For each trajectory, we were able to classify, using machine learning on the behavioral data, which of the mechanisms (persistence or adaptation) was dominant. An involvement of the insula and bilateral IPS was found when persistence dominated, supporting the hypothesis of differential network recruitment/interaction for the two mechanisms. Such effect is consistent with a role for the ventral attentional network. This study adds to the understanding of perceptual multistability and gives a better insight into the underlying causes of the perceptual hysteresis phenomenon.

2. Methods

2.1. Participants

Twenty-five healthy participants were recruited for this experiment (13 male, mean age 28.4 ± 3.2 years). All had normal or corrected-to-normal vision and no history of neurological or psychiatric diseases. All participants except one were right-handed, as confirmed by a handedness questionnaire adapted from (Oldfield, 1971): mean laterality index of 87.7 ± 10.5. All gave informed written consent before participating, in accordance with the declaration of Helsinki, and the study followed the safety guidelines for magnetic resonance imaging research on humans. The work was approved by the Ethics Committee of the Faculty of Medicine of the University of Coimbra.

2.2. Experimental setup

The acquisition session comprised one structural magnetic resonance imaging (MRI) sequence and eight functional MRI (fMRI) sequences (four control runs, and four testing runs – Fig. 1A). The control runs allowed us to establish a relation, without the contribution of perceptual history, between controlled stimulus variables and the perceptual report, while the testing runs assessed perceptual history mechanisms and their contribution to hysteresis. The stimulus was created in MATLAB R2016b (The Mathworks, Inc., Natick, MA-USA), along with the Psychophysics Toolbox version 3 (Pelli, 1997; Brainard, 1997), and was presented on an LCD screen (70 × 39.5 cm, 1920 × 1080 pixel resolution, 60 Hz refresh rate) which the participants viewed through a mirror mounted above their eyes at an effective distance of 156 cm. Participants' reports were recorded using a fiber-optical MR-compatible response box (Cedrus Lumina LSC-400B). To confirm whether participants maintained central fixation during the acquisition session, individually calibrated eye-tracking data (sample frequency of 500 Hz) were recorded inside the scanner using Eyelink 1000 software (SR Research, Ottawa, Ontario, Canada).

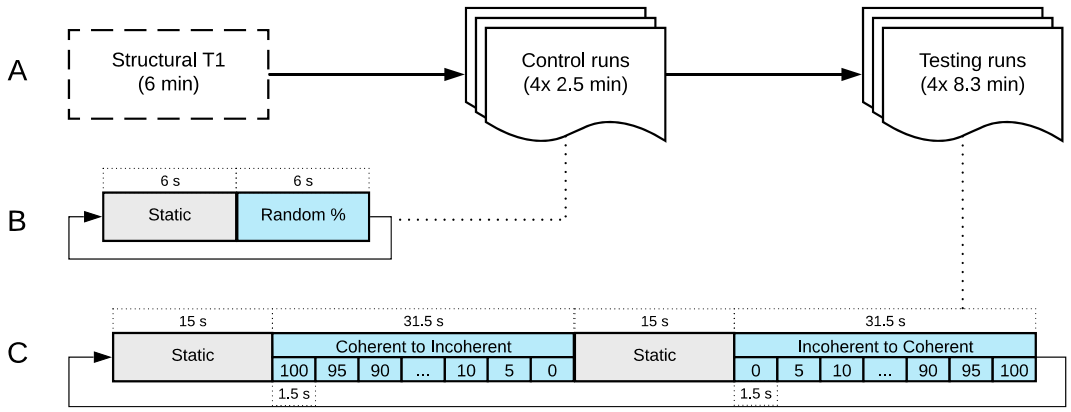

Fig. 1. Experimental protocol design. A) Diagram of the scanning session. B) Protocol scheme of each trial of the control runs. C) Protocol scheme of each trial of the testing runs. The stimulus properties were manipulated, in the testing runs, by gradually changing the level of coherence from 0% to 100 % or from 100% to 0%. In the control runs, the various levels were displayed randomly.

2.2.1. Stimulus

We used a moving plaid (superposition of two moving gratings – Fig. 2A), which can be perceived moving coherently (Fig. 2B) or incoherently (Fig. 2C), and as such, the stimulus is intrinsically ambiguous.

The observer's tendency to perceive coherence has been manipulated systematically through many parameters (Movshon et al., 1985; Adelson and Movshon, 1982). Here, to force the perception of one of the two possible motion interpretations, we added dots to the plaid to disambiguate motion (Fig. 2D). Depending on the relative percentage of dots (superimposed on the bars) that move vertically or horizontally, we were able to induce a given level of coherence, hence a perceptual interpretation to the participant (see the control and testing runs description below for more details). With 100% of the dots moving vertically (down), the coherent percept is induced, while with 100% of the dots moving horizontally (half to the left and half to the right), the incoherent percept is induced.

A complete description of the stimulus properties is provided in Table 1, matching our previous study (Sousa et al., 2018).

Table 1
Plaid stimulus properties.

Angle of gratings relative to horizontal (°)	65
Duty cycle (%)	25
Aperture diameter (° visual angle)	9
Screen background color (RGB)	(0, 0, 0)
Plaid background color (RGB)	(50, 50, 50)
Gratings color (RGB)	(130, 130, 130)
Spatial frequency (cycle/° visual angle)	0.625
Motion speed (° visual angle/s)	1.6
Number of dots	800
Dots color (RGB)	(20, 20, 20)
Dots size (° visual angle)	0.05
Dots horizontal speed (° visual angle/s)	2.4
Dots vertical speed (° visual angle/s)	4
Fixation cross width (° visual angle)	0.67

2.2.2. Control runs

The control runs consisted of 6-s blocks of the static plaid interleaved with blocks of the moving plaid (Fig. 1B). In each motion block, the plaid was overlaid with moving dots. Depending on the coherence level desired, the number of dots moving horizontally or vertically was changed. Each level (from 0 to 100% in intervals of 10% - totaling 11 levels) was presented once per run, in random order. The participants were instructed to look at the central fixation cross and report, by pressing and holding one of two buttons, the current percept of motion (coherent or incoherent) while the plaid was moving.

This continuous report allowed us to establish the relationship between the parametric manipulations of the stimulus (level of coherence) and the observer's perception, without the contribution of recent

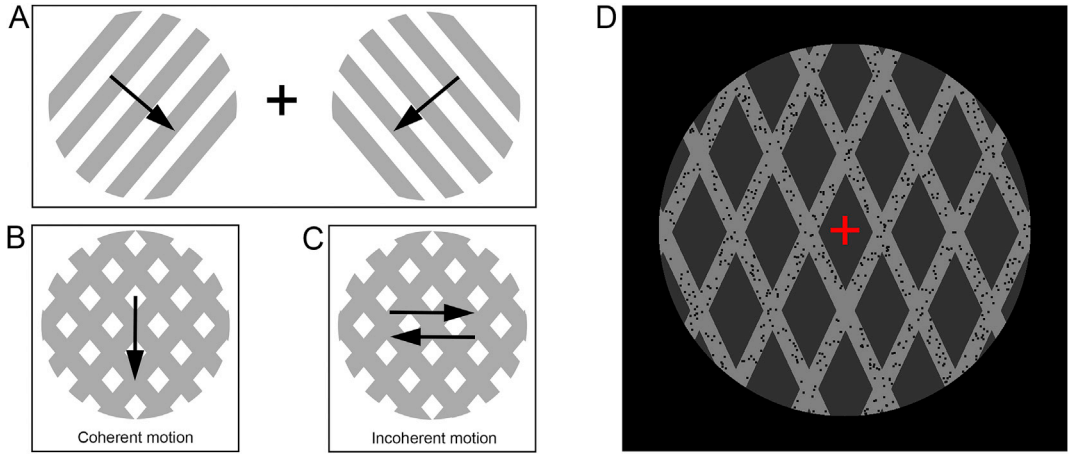

Fig. 2. Stimuli used in the experiment. Panels A, B, and C illustrate a plaid stimulus. By superimposing two gratings (A), moving orthogonally to the lines, a bistable stimulus is created, which can be perceived moving coherently (B) as a single surface or incoherently (C) as two separate surfaces sliding over each other. Arrows illustrate the direction of perceived motion. D) Type of Plaid stimulus used in the experiment. Depending on the moving dots' direction, the otherwise ambiguous stimulus was perceived as a plaid moving coherently or incoherently.

perceptual history. The average report curve of the four runs is used as a robust control for the perceptual trajectories during the testing runs.

2.2.3. Testing runs

The testing runs consisted of two motion conditions - one in which the plaid gradually transitions from Coherent to Incoherent and the other from Incoherent to Coherent - interleaved with a static condition (Fig. 1C). During the motion blocks, which last for 31.5 s, the level of coherence was gradually changed (steps of 5%) from 0 to 100% (in the Incoherent to Coherent condition) and from 100% to 0% (in the Coherent to Incoherent condition). Participants were instructed to look at the central fixation cross and continuously report the current percept by pressing and continuously holding one of the two buttons of the response box. In each run, we had four blocks of each of the conditions.

2.3. fMRI data acquisition

Scanning was performed on a 3T Siemens Magnetom Tim Trio scanner at the Institute of Nuclear Sciences Applied to Health (ICNAS), Portugal, using a 12-channel head coil. The scanning session started with the acquisition of one 3D anatomical magnetization-prepared rapid acquisition gradient echo (MPRAGE) pulse sequence (TR = 2530 ms, echo time (TE) = 3.42 ms, flip angle = 7°, 176 slices, voxel size = 1.0 × 1.0 × 1.0 mm, field of view (FOV) = 256 × 256 mm). Afterward, eight functional runs were acquired using a T2*-weighted gradient echo-planar imaging (EPI) sequence. These consisted of 100 volumes in the control runs and 266 volumes in the subsequent runs (TR = 1500 ms, TE = 30 ms, flip angle = 75°, 27 interleaved slices without gap, voxel size = 3.5 × 3.5 × 3.5 mm, FOV = 235 × 235 mm). In total, the scanning session lasted 45 min.

2.4. fMRI data processing

Data processing was performed using BrainVoyager v20.6 (Brain Innovation, The Netherlands), automated using custom MATLAB scripts. Pre-processing included slice-scan time correction, 3D head-motion correction, temporal high-pass filtering (GLM-Fourier, 2 cycles), and spatial smoothing with a Gaussian filter of FWHM = 6 mm. Data were normalized to Talairach space (Talairach and Tournoux, 1988). Activation maps were created using a General Linear Model (GLM), with predictors for each experimental condition and confound predictors from six detrended head motion parameters (3 translation, 3 rotation) and spikes (Satterthwaite et al., 2013).

2.5. Behavioral data analysis

The perceptual reports were acquired via button presses (continuous hold for a given perceptual state) with a temporal resolution of 60 Hz, enabling the detection of changes at the level of single stimulus frames. These were then used to label the perceptual state corresponding to each block of 1.5 s (which matches the volume duration and the step of coherence change). We calculated the percentage of "Coherent" reports over the total number of reports for each volume (which corresponded to a certain coherence level of the stimulus), allowing us to trace a perceptual report curve for the three motion conditions (Control – no history, transition from Coherent to Incoherent, and from Incoherent to Coherent).

The reports of the control runs were averaged for each subject. This allowed us to trace a subject-specific control curve which accurately revealed how the coherence level of the plaid related to the perceived motion in the absence of perceptual history.

The reports of the testing runs were analyzed per run. Given the nature of bistable dynamical systems, we did not expect that the competition between persistence and adaptation mechanisms would have the same outcome every time, which is also the case for other bistability examples such as binocular rivalry and Necker Cube perception. Hence, we avoided averaging runs in this case, which would occlude the dynamics of perceptual rivalry.

2.5.1. Perceptual history effects: hypotheses

We hypothesized four distinct effects on the perceptual reports of each trajectory due to recent perceptual history, as illustrated in Fig. 3. When the transition to the opposing percept occurs later, as compared with the control curve, the effect is *positive hysteresis*, reflecting a dominant persistence mechanism; if the transition occurs earlier, the effect is *negative hysteresis*, reflecting a dominant adaptation mechanism; if no visible difference between the testing and the control curve exists, the effect is *Null*, i.e., the two mechanisms cancel each other; if the effect on the testing curve is not clear, i.e., the transition to the opposing percept seems, for example, to occur earlier (when compared to the control curve) but then this effect is modified (sometimes resembling the opposite effect), the effect is labeled *Undefined*.

2.5.2. Perceptual history effects: classification

Based on the hypotheses defined above, we classified the collected behavioral data in four groups: positive and negative hysteresis, null, and undefined. This classification was initially based on visual inspection. Then, an automatic classification algorithm was implemented to test the groups' validity.

A mathematical model, which allowed the creation of simulated keypress response curves, was defined to train the classifier. The main equation of the model, which returns the probability of perceiving coherent motion, $P_{coh}(t)$, is:

$$P_{coh}(t) = \frac{1}{1 + e^{-30[x(t)-(d+w(t)+\varepsilon)]}} \quad (1)$$

where $x(t)$ is the fraction of dots moving down, d the control curve inflection (transition) point, ε white random noise, and $w(t)$ the weight of the recent perceptual history, which varies according to the chosen effect to simulate. As Supplementary Material, we provide a complete description of the model and a schematic representation of the automatic classification pipeline (Figure S1).

For each perceptual trajectory (Coherent to Incoherent and Incoherent to Coherent), 300 simulated curves per class were generated. Two features were extracted from the perceptual report curves: the first feature is the difference between the area under curve (AUC) of the control and test curves, centered on the control transition value (5-point window), divided by the total area under both curves; the second feature is the difference between the perceptual switches of control and test curves. The features were then normalized between 0 and 1, by subtracting the minimum value of the feature and dividing by its maximum.

The features extracted from the simulated dataset were then used to train a Bayes naive classifier (MATLAB implementation using *fitcnb* function with default parameters, from the Statistics and Machine Learning Toolbox), based on 10-fold cross-validation. Afterward, the same features were extracted from the test dataset, composed of real reports data, and normalized using the same method, but with the train dataset parameters. The classifier returned a predicted label for all 100 trials of the test dataset. We repeated the whole classification process 10 times to account for the noise added to the simulation. We then extracted the most frequent predicted label for each testing sample, from which we computed a confusion matrix. The final classification accuracy was calculated as the average of the four *one-against-all* balanced accuracies for each class.

2.6. fMRI data analysis

2.6.1. Control runs

The control runs consisted of very short blocks of moving and static plaids. We considered all motion conditions and used these runs as a functional localizer of the network involved in visual motion perceptual decision.

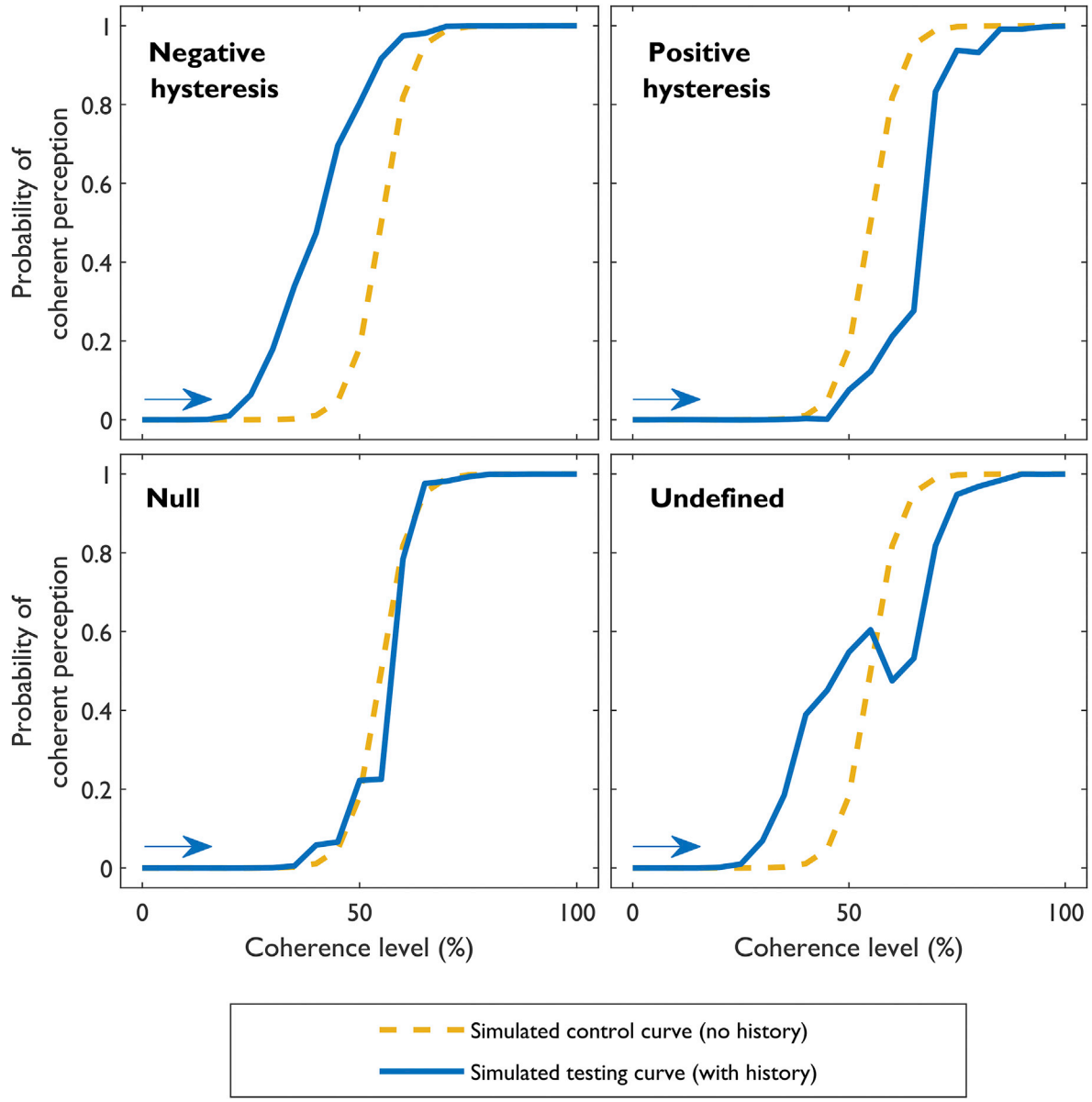

Fig. 3. Graphical representation of the perceptual history effects considered. Each plot represents the hypothesized effects of perceptual history on the reports of a trajectory (we show single incoherent-coherent trajectories only, for simplicity), visible from the differential shift and shape of the testing curves (in blue) when compared to the control curve (in yellow). The control curves represent the relation between the coherence level and the probability of coherent perception in the absence of history.

A random-effects (RFX) GLM analysis was performed considering all control runs and contrasting Motion vs. Static conditions. The resulting activation map (Bonferroni-corrected at $p = 0.05$) allowed us to explore and define the regions involved in interpreting the moving plaid pattern of motion, including our two main regions of interest - hMT+ and insula (given the controversy on lateralization we analyzed the left and right insula separately).

2.6.2. *Testing runs*

For the analysis of the testing runs, we integrated information of the perceptual reports taking into account that the effect of previous experience is most evident before the perceptual switch to the opposing percept.

For each run, we used the perceptual transition volume to define what we designated by *effect block*. This block is composed of this volume and the four volumes before it. If the perceptual switch occurred very early, we excluded the first volume of the condition block and considered the following five as *effect block*. We created predictors for this effect block by convolving a standard Hemodynamic Response Function (HRF) with the box-car time-course of the effect block condition. Then, an ROI-GLM analysis was performed, from which we extracted the beta values of the *effect block* from the regions defined, for each run and each participant, when contrasted with the baseline condition.

Considering the most evident perceptual history effect in each trajectory, we compared the beta values between the positive and negative hysteresis, irrespective of the experimental condition (Coherent to Incoherent or the opposite). We applied a two-way ANOVA, with a factor for the perceptual history effect and another for the brain regions, as implemented in MATLAB. Following unpaired t-tests, comparing the two effects in each brain region, were performed and corrected for the six regions using Bonferroni's method.

Additionally, as a confirmatory analysis, we subsampled the dataset only considering runs where the two effects were found. This allowed for a new two-way ANOVA, followed by paired t-tests between the two

effects in each region. These results were also corrected using Bonferroni's method.

2.7. Code availability

The code for all analyses performed is available at our lab's GitHub page https://github.com/CIBIT-ICNAS/public_vphysteresis.

3. Results

3.1. Behavioral results

3.1.1. Perceptual reports

Participants were instructed to report the perceived type of motion continuously (by holding a button constantly for each perceptual state) while the plaid was moving. This allowed us to calculate the percentage of coherent reports at each volume and plot it against the variable of interest, the coherence level. In Fig. 4, we show four examples of the perceptual report time-courses.

From these curves, one can infer the effect of perceptual history for each trajectory. Positive hysteresis is evident for the blue curves in both examples (later transition to the opposite percept when comparing with the control curve) while negative hysteresis is evident for the red curve in panel A (earlier transition to the opposite percept), but not in panel B. In this case, the effect is null (no difference to the control curve).

The example in panel A illustrates a novel asymmetric perceptual hysteresis profile, where different neural mechanisms dominate for each trajectory. In fact, the persistence mechanism was mainly evident in the Incoherent to Coherent trajectory (leading to positive hysteresis), while adaptation was in the opposite trajectory (leading to negative hysteresis), as explained in the next section 3.1.2.

3.1.2. Classification of perceptual history effects

Behavioral data were classified into four groups according to the perceptual history effect. Based on the visual classification of each curve (trajectory), comparing with the hypotheses of Fig. 3, we found 50 cases of negative hysteresis (47 in the coherent to incoherent transition and 3 in the opposite one), 60 cases of positive hysteresis (48 in the incoherent to coherent transition and 12 in the opposite one), 40 cases of no evident perceptual history effect (20 in the coherent to incoherent transition and 20 in the opposite one) and 50 cases in which the perceptual history effect was undefined (29 in the incoherent to coherent transition and 21 in the opposite one). Moreover, positive and negative hysteresis cases were trajectory-dependent, with the strongly adapting coherent-starting trajectory leading to negative hysteresis and the weakly adapting incoherent-starting trajectory leading to positive hysteresis (chi-square statistic with Yates correction, 57.117, $p < 0.001$).

The automatic classification process validated the groups' distribution, discriminating between effects with a balanced accuracy of 81.4% and 80.1% for the Coherent to Incoherent and Incoherent to Coherent transitions, respectively (Fig. 5). As shown in the confusion matrices, the Undefined and Null effects present the highest number of cases in which the automatic classification and the visual inspection criteria did not match.

3.2. Neurophysiological results: fMRI data analysis

3.2.1. The neural network involved in visual motion perceptual decision

The control runs were used as a localizer for our regions of interest - insula and hMT+ - as well as for additional regions that are part of the network involved in perceptual decision making. Fig. 6 displays the group activation map, when contrasting motion vs. static conditions: we identified visual areas related to motion processing (hMT+ and V3A), the

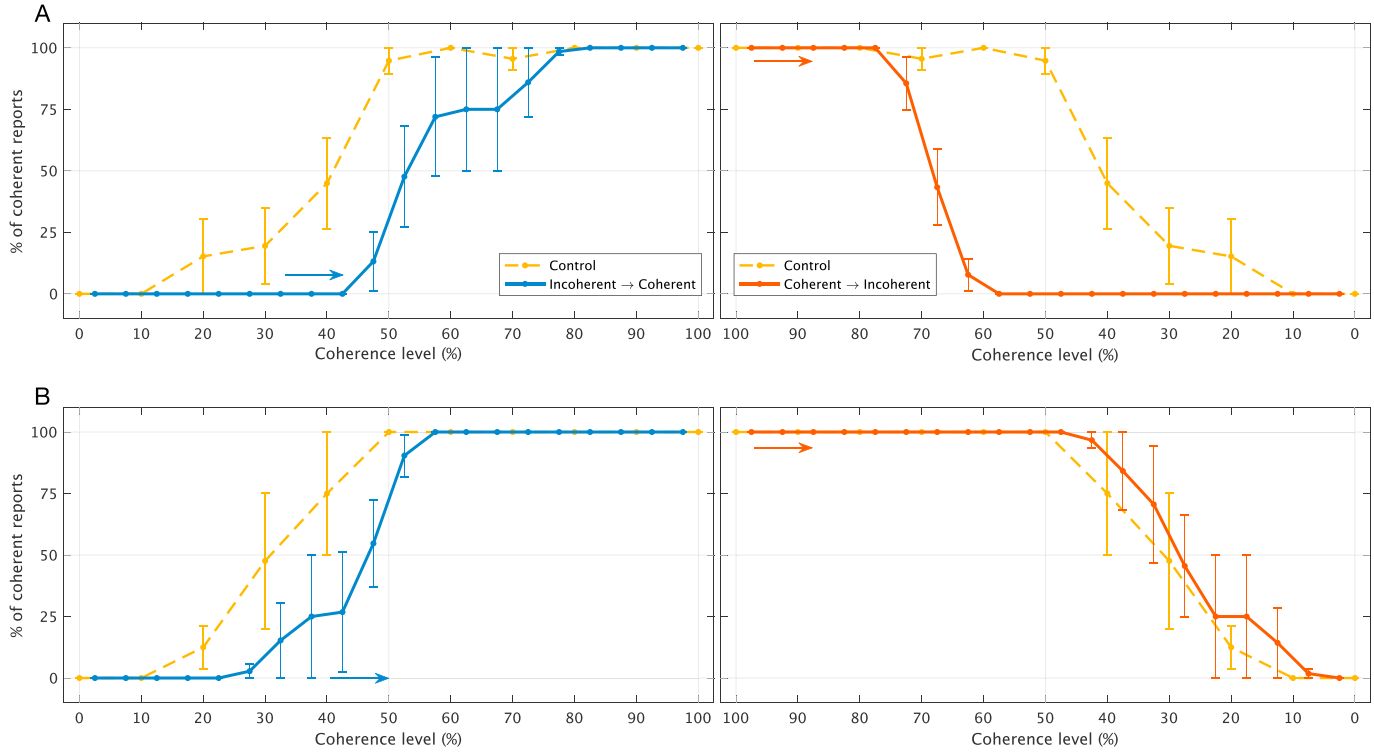

Fig. 4. Perceptual report time-course examples from two different participants (A and B). The horizontal axis displays the variable which we manipulated, the coherence level, and the vertical axis displays the percentage of coherent reports by the participant. The control curves, in yellow, show the relation between the two variables when the effect of history is not present. The reports for the Incoherent to Coherent trajectory (from 0 to 100% of coherence) are shown in blue on the left-side plots. On the right-side plots, in orange, we display the reports for the Coherent to Incoherent trajectory (from 100 to 0% of coherence). Error bars display the standard error of the mean.

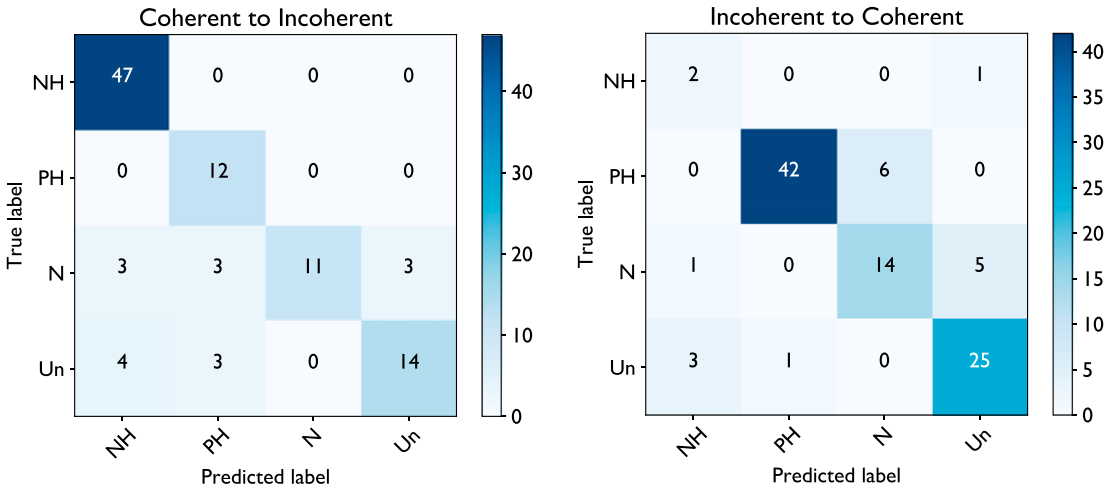

Fig. 5. Classification of perceptual history effects. Classification confusion matrices for both experimental trajectories (left matrix - Coherent to Incoherent, right matrix - Incoherent to Coherent). The number of cases equally classified by visual inspection and the automatic classifier is shown in the matrices' main diagonal, for each of the four effects: Negative hysteresis (NH), Positive hysteresis (PH), Null (N) and Undefined (Un). The colorbar represents the number of cases.

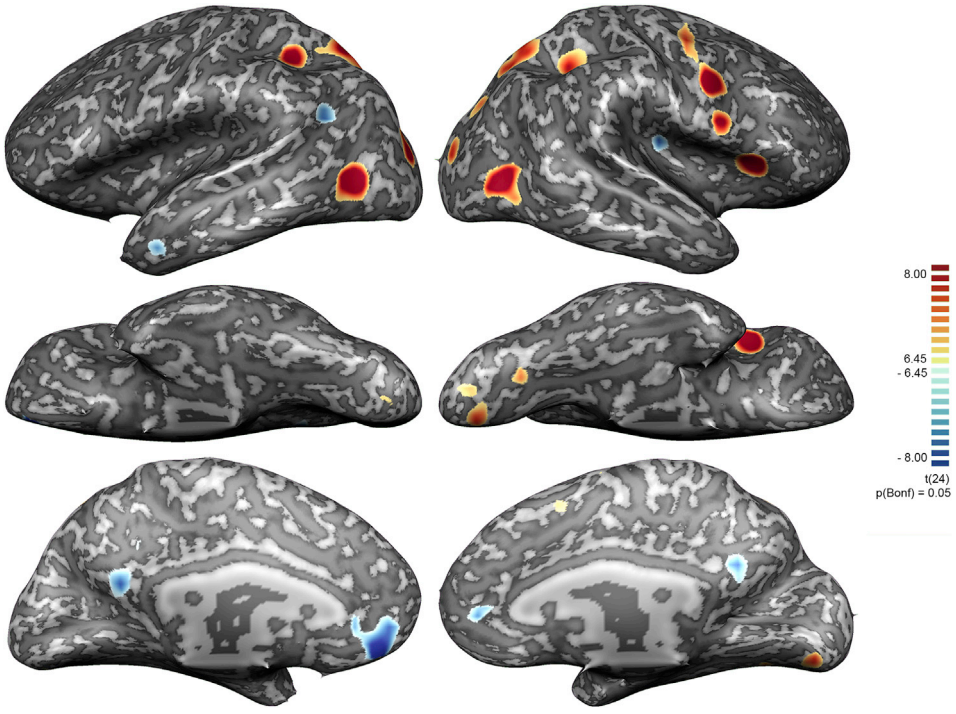

Fig. 6. RFX-GLM activation map of the control runs. The map contrasts motion vs. static conditions, Bonferroni corrected at $p = 0.05$. The contrast reveals the network of regions involved in the visual motion perceptual decision task, including our regions of interest: insula and hMT+.

superior parietal lobe (SPL), the intraparietal sulcus (IPS), the frontal eye fields (FEF), the premotor cortex (PMC), the supplementary motor area (SMA), and the insula. The Talairach coordinates of these brain regions are summarized in Table S2.

3.2.2. *Perceptual adaptation versus persistence*

We analyzed the fMRI testing runs to assess the activation level of the network regions when the perceptual history effect is most evident (*effect block*). For this analysis, we considered all regions bilaterally, while taking into account prior evidence for lateralization of the insula, and excluded the button press-related motor regions (FEF, PMC, and SMA). In sum, we have six regions (left and right insula, bilateral hMT+, SPL, IPS, and V3A) and two perceptual history effects.

A two-way ANOVA revealed that there was a significant main effect of the perceptual history effect (our main hypothesis) on brain activation, $F(1,648) = 21.1$, $p < 0.001$, and also a significant main effect of brain region, $F(5,648) = 25.3$, $p < 0.001$. Importantly, Bonferroni's multiple comparisons tests showed that brain activation was significantly higher for persistence than for adaptation for the right insula ($p = 0.035$, 95% CI of the difference $= -0.275$ to -0.006, correcting for the six brain regions) (Fig. 7). The ANOVA table and multiple comparison test results are provided as Supplementary Material (Table S4 and S5, respectively).

The ANOVA on the subsampled dataset confirmed the statistical significance of both main effects (brain region: $F = 16.8$, $p = 0.713$; perceptual history effect: $F = 14.7$, $p < 0.001$), and the following paired testing showed statistically significant differences for the right Insula (p

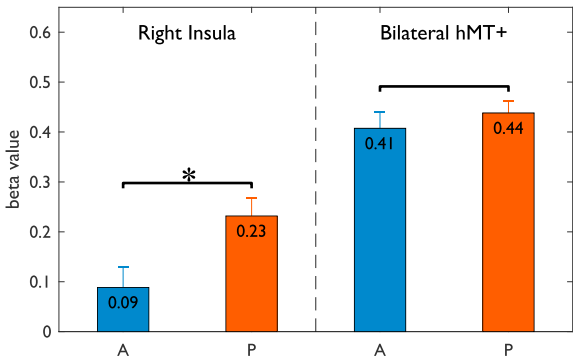

Fig. 7. Differences in ROI activity between perceptual persistence and adaptation mechanisms. Comparison between the ROI beta values of the *effect block* predictor of the adaptation (A) and persistence (P) groups. The bars represent the average beta value together with the standard error of the mean. Statistical testing was performed using a two-way ANOVA followed by Bonferroni's multiple comparison tests (*$p \leq 0.05$).

= 0.002, 95% CI of the difference = −0.256 to −0.082), left Insula (p = 0.044, 95% CI of the difference = −0.208 to −0.035), and bilateral IPS (p = 0.018, 95% CI of the difference = −0.230 to −0.051). The ANOVA table and full paired test results are provided as Supplementary Material (Table S6 and S7, respectively).

4. Discussion

In this study, we explored the neural mechanisms underlying perceptual hysteresis, testing the hypothesis of a critical balance between persistence and adaptation, the key mechanisms underlying positive and negative hysteresis, respectively. To address this question, we used a bistable motion perception paradigm. We asked whether there is hysteresis in the perceptual transition between opposing percepts of a moving plaid (coherent vs. incoherent) and studied the neural correlates underlying this phenomenon, combining behavioral and fMRI data. Data were acquired while participants reported their perceptual interpretation of a moving plaid, gradually changing its pattern of motion from coherent to incoherent and from incoherent to coherent.

The behavioral results show how recent experience influences the current perception of each stimulation trajectory. When compared to the absence of history, the perceptual switch might occur later (positive hysteresis, evidence for persistence) or earlier (negative hysteresis, evidence for adaptation). We also found cases where previous experience did not seem to exert an obvious or unique influence on perceptual interpretation (null and undefined effects).

Perceptual hysteresis has been initially associated with a persistence mechanism only, but currently, there is evidence that it may also be related to adaptation, causing negative hysteresis (Liaci et al., 2018). It has been debated whether positive and negative hysteresis arise from a single mechanism with different outputs (Gepshtein and Kubovy, 2005) or from two dedicated mechanisms (Wilson, 2007; Wilson, 2017; Lopresti-Goodman et al., 2013). Nevertheless, the most recent studies about the influence of history on perceptual decision support the hypothesis of two opposing mechanisms with distinct effects (Schwiedrzik et al., 2014; Fritsche et al., 2017; Liaci et al., 2018). Moreover, there is evidence for competition between both mechanisms. (Kleinschmidt et al., 2002) have reported a hysteresis-related phenomenon, which effectively reversed the adaptation-associated deactivation of the ventral lateral occipital cortex. Later, (Buckthought et al., 2008) showed that a stronger adaptation could reduce the positive hysteresis effects. Our results agree with this competition hypothesis since all perceptual history effects found reveal the possible outcomes of such a competition between persistence and adaptation mechanisms: a dominance of persistence or adaptation (positive or negative hysteresis), a no clear winner (undefined effect), or a draw (null effect).

Our data add to the debate over the nature of positive and negative perceptual hysteresis. Perceptual hysteresis has been commonly applied as a synonym of perceptual persistence (Buckthought et al., 2008; Hock et al., 1993; Schwiedrzik et al., 2014). However, a control task is needed to understand whether the perceptual switch occurs earlier or later than without history. We argue that we can only infer the neural mechanism behind perceptual hysteresis when comparing with a case in the absence of history. This is particularly relevant to asymmetric perceptual curves. As a major novelty of our study, we showed evidence for different dominant mechanisms influencing each trajectory, which can then lead to these asymmetric hysteresis profiles.

In a recent behavioral study (Liaci et al., 2018), the authors performed a detailed analysis of the hysteresis phenomenon with two different paradigms. They found evidence for positive and negative hysteresis, but the control curve was always between both testing curves (the mechanism affecting both trajectories was the same). Strikingly, we found cases in which the control curve was not between the two testing curves (see examples of Fig. 4), which illustrate the hypothesis of a novel hysteresis profile resulting from the combination of mechanisms affecting each trajectory. Our data are consistent with the notion that positive hysteresis is the result of a stronger persistence mechanism overall, while negative hysteresis results from a stronger adaptation mechanism (Liaci et al., 2018).

The competition between perceptual history mechanisms did not have the same outcome every time, as expected, given the inherent nature of bistable dynamical systems. The automatic classification step of the behavioral reports allowed us to validate the visual classification based on graphical outputs. By comparing the results of both types of classification, automatic and manual, we show that each trajectory was labeled reliably. The results showed that positive hysteresis occurred mainly in the perceptual transition from incoherent to coherent motion, while negative hysteresis occurred mainly in the perceptual transition from coherent to incoherent motion, which is consistent with the notion that adaptation is stronger for coherent motion (Sousa et al., 2018) - persistence dominates when the level of adaptation is lower.

Neuroimaging data allowed us to identify the neural correlates of perceptual hysteresis and to confirm that hMT+ and the insula are involved in regulating the perceptual history effect. Firstly, our results show a significantly higher activity of the insula during persistence when compared to adaptation. Importantly, we verified that this difference in activation was not due to the distinct average coherence level of the plaid found for the two mechanisms (Figure S2). The anterior insula is a core region of the ventral attention network (Eckert et al., 2009; Uddin, 2014; Zhang et al., 2018). Moreover, as part of the salience network, it is found to be associated with evidence accumulation and perceptual decision-making (Sterzer and Kleinschmidt, 2010; Rebola et al., 2012; Duarte et al., 2017). The fact that it is a hub of the salience network, linking bottom-up processes to the brain's attentional and working memory resources (Menon and Uddin, 2010), provides a substrate for the persistence mechanism identified here.

Secondly, the insula activity difference between mechanisms was more strongly present in the right hemisphere (although a significant effect for the left insula was also found in the confirmatory analysis). The salience and ventral attention networks play an important role here (Corbetta and Shulman, 2002; Sheremata et al., 2010; Sheremata and Silver, 2015), indicating that perception-driven attention, and its link to short memory substrates, provide the basis for neural and behavioral perceptual persistence. An earlier study, with a paradigm based on an intermittent presentation of rectangular dot lattices, addressed adaptation and hysteresis while regarding the latter as a synonym of persistence (Schwiedrzik et al., 2014). This study did not investigate the balance between mechanisms (the paradigm does not allow to critically test competition between hysteresis mechanisms) but suggested that fronto-parietal regions have a key role in perceptual stabilization. Our results are consistent with this hypothesis and add to the debate over the role of high-level regions in perceptual decision and hysteresis (Kleinschmidt et al., 2002).

We note, as a limitation, that the intrinsically high variability of the perceptual dynamics, even at the single-subject level, posed a challenge for statistical analyses, while managing the balance between Type I and Type II errors. We avoided averaging different effects, which would be suboptimal for an effective analysis of such a dynamical system - this is generally the case for other examples of bistability as well. Still, a confirmatory analysis was performed, based only on the available paired samples, that revealed additional significant differences for the left anterior insula and bilateral IPS between the two mechanisms. Although a larger effect still stands for the right anterior insula, the left insula and the IPS also seem to play a role, as corroborated by the absence of interaction between perceptual mechanism and brain region factors.

Finally, we have previously shown that coherent and incoherent patterns of motion lead to distinct perceptual adaptation strengths and that this mechanism originates at an early level (hMT+) even when the net activity remains unchanged (Sousa et al., 2018). The observation of neural adaptation was related to both percepts of motion, but it was stronger in the case of coherent perception, which supports, as stated above, the evidence for a winning adaptation mechanism on the transition from coherent to incoherent perception.

In summary, our results show evidence for continuous competition between perceptual history mechanisms. For each trajectory, we were able to classify which mechanism was dominant and conclude that a stronger involvement of the insula was found when persistence dominated, supporting the hypothesis of differential network recruitment/interaction for the two mechanisms. The results of this study show important implications for understanding multistable perception and give a better insight into the underlying causes of perceptual hysteresis.

Declaration of competing interest

The authors declare no competing interests.

CRediT authorship contribution statement

Alexandre Sayal: Conceptualization, Methodology, Software, Investigation, Formal analysis, Writing - original draft, Writing - review & editing. **Teresa Sousa:** Conceptualization, Methodology, Investigation, Formal analysis, Writing - original draft, Writing - review & editing. **João V. Duarte:** Conceptualization, Methodology, Formal analysis, Writing - review & editing. **Gabriel N. Costa:** Conceptualization, Methodology, Formal analysis, Writing - review & editing. **Ricardo Martins:** Methodology, Conceptualization, Software, Writing - review & editing. **Miguel Castelo-Branco:** Conceptualization, Methodology, Writing - review & editing, Supervision.

Acknowledgments

We would like to thank the participants for their involvement in this study. We are also grateful to Carlos Ferreira and Sónia Afonso for the help with fMRI setup and scanning. This research work was funded by the Portuguese Foundation for Science and Technology (FCT) (COMPETE UID/04950/2020, Centro 2020 (BIGDATIMAGE - CENTRO-01-0145-FEDER-000016), POCI-01-0145-FEDER-030852, PCIF/SSO/0082/2018 and by the BIAL Foundation, Portugal (projects 207/16 and 258/18).

Appendix A. Supplementary data

Supplementary data to this article can be found online at https://doi.org/10.1016/j.neuroimage.2020.117153.

References

Adelson, Edward H., Movshon, J. Anthony, 1982. Phenomenal coherence of moving visual patterns. Nature 300 (5892). https://doi.org/10.1038/300523a0.

Anstis, S., Kim, J., 2011. Local versus global perception of ambiguous motion displays. J. Vis. https://doi.org/10.1167/11.3.13.

Assad, J.A., Hacohen, N., Corey, D.P., 1989. Voltage dependence of adaptation and active bundle movement in bullfrog saccular hair cells. Proc. Natl. Acad. Sci. Unit. States Am. 86 (8), 2918–2922. https://doi.org/10.1073/pnas.86.8.2918.

Babu, H. Aswath, Wanare, Harshawardhan, 2011. Negative and positive hysteresis in double-cavity optical bistability in a three-level atom. Phys Rev A - Atomic, Molecular, and Optical Phys 83 (3). https://doi.org/10.1103/PhysRevA.83.033818.

Brainard, D.H., 1997. The Psychophysics Toolbox. Spatial Vis. 10 (4), 433–436. https://doi.org/10.1163/156856897X00357.

Brascamp, Jan, Sterzer, Philipp, Blake, Randolph, Knapen, Tomas, 2018. Multistable perception and the role of frontoparietal cortex in perceptual inference. Annu. Rev. Psychol. 69 (1) https://doi.org/10.1146/annurev-psych-010417-085944 annurev-psych-010417-085944.

Buckthought, Athena, Kim, Jeounghoon, Wilson, Hugh R., 2008. Hysteresis effects in stereopsis and binocular rivalry. Vis. Res. 48 (6), 819–830. https://doi.org/10.1016/j.visres.2007.12.013.

Castelo-Branco, Miguel, Formisano, Elia, Backes, Walter, Zanella, Friedhelm, Neuenschwander, Sergio, Singer, Wolf, Goebel, Rainer, 2002. Activity patterns in human motion-sensitive areas depend on the interpretation of global motion. Proc. Natl. Acad. Sci. U.S.A. 99 (21), 13914–13919. https://doi.org/10.1073/pnas.202049999.

Corbetta, Maurizio, Shulman, Gordon L., 2002. Control of goal-directed and stimulus-driven attention in the brain. Nat. Rev. Neurosci. https://doi.org/10.1038/nrn755.

Duarte, João Valente, Costa, Gabriel Nascimento, Martins, Ricardo, Castelo-Branco, Miguel, 2017. Pivotal role of hMT+ in long-range disambiguation of interhemispheric bistable surface motion. Hum. Brain Mapp. 38 (10), 4882–4897. https://doi.org/10.1002/hbm.23701.

Eckert, Mark A., Menon, Vinod, Adam, Walczak, Ahlstrom, Jayne, Stewart, Denslow, Horwitz, Amy, Judy, R., Dubno, 2009. At the heart of the ventral attention system: the right anterior insula. Hum. Brain Mapp. 30 (8), 2530–2541. https://doi.org/10.1002/hbm.20688.

Frackowiak, Richard S.J., Friston, Karl J., Frith, Christopher D., Dolan, Raymond J., Price, Cathy J., Zeki, Semir, Ashburner, John T., Penny, William D., 2004. Perceptual construction. In: Human Brain Function, second ed. Academic Press, pp. 47–60.

Fritsche, Matthias, Mostert, Pim, de Lange, Floris P., 2017. Opposite effects of recent history on perception and decision. Curr. Biol. 27 (4), 590–595. https://doi.org/10.1016/j.cub.2017.01.006.

Gepshtein, Sergei, Kubovy, Michael, 2005. Stability and change in perception: spatial organization in temporal context. Exp. Brain Res. 160 (4), 487–495. https://doi.org/10.1007/s00221-004-2038-3.

Gigante, Guido, Mattia, Maurizio, Braun, Jochen, Del Giudice, Paolo, 2009. Bistable perception modeled as competing stochastic integrations at two levels. PLoS Comput. Biol. 5 (7), 1–9. https://doi.org/10.1371/journal.pcbi.1000430.

Hock, Howard S., Scott Kelso, J., Schöner, Gregor, 1993. Bistability and hysteresis in the organization of apparent motion patterns. J. Exp. Psychol. Hum. Percept. Perform. 19 (1), 63–80. https://doi.org/10.1037/0096-1523.19.1.63.

Hock, Howard S., Schöner, Gregor, 2010. Measuring perceptual hysteresis with the modified method of limits: dynamics at the threshold. Seeing Perceiving 23 (2). https://doi.org/10.1163/187847510X503597.

Hock, Howard S., Schöner, Gregor, Voss, Audrey, 1997. The influence of adaptation and stochastic fluctuations on spontaneous perceptual changes for bistable Stimuli. Percept. Psychophys. https://doi.org/10.3758/BF03211860.

Huguet, Gemma, Rinzel, John, Hupé, Jean-Michel, 2014. Noise and adaptation in multistable perception: noise drives when to switch, adaptation determines percept choice. J. Vis. https://doi.org/10.1167/14.3.19.

Huk, Alexander, Heeger, David, 2002. Pattern-motion responses in human visual cortex. Nat. Neurosci. 5 (1), 72–75. https://doi.org/10.1038/nn774.

Kleinschmidt, Andreas, Büchel, Christian, Hutton, Chloe, Friston, Karl J., Frackowiak, Richard S.J., 2002. The neural structures expressing perceptual hysteresis in visual letter recognition. Neuron 34 (4), 659–666. https://doi.org/10.1016/S0896-6273(02)00694-3.

Lamichhane, Bidhan, Adhikari, Bhim M., Dhamala, Mukesh, 2016. The activity in the anterior insulae is modulated by perceptual decision-making difficulty. Neuroscience. https://doi.org/10.1016/j.neuroscience.2016.04.016.

Laval, Jorge A., 2011. Hysteresis in traffic flow revisited: an improved measurement method. Transp. Res. Part B Methodol. 45 (2), 385–391. https://doi.org/10.1016/j.trb.2010.07.006.

Liaci, Emanuela, Fischer, Andreas, Atmanspacher, Harald, Heinrichs, Markus, Tebartz van Elst, Ludger, Kornmeier, Jürgen, 2018. Positive and negative hysteresis effects for the perception of geometric and emotional ambiguities. PloS One 13 (9), 1–32. https://doi.org/10.1371/journal.pone.0202398.

Lopresti-Goodman, Stacy M., Turvey, Michael T., Frank, Till D., 2013. Negative hysteresis in the behavioral dynamics of the affordance “graspable”. Atten. Percept. Psychophys. 75 (5), 1075–1091. https://doi.org/10.3758/s13414-013-0437-x.

Lorent, Pacp, Davidenko, Jorge, 1990. Hysteresis phenomena in excitable cardiac tissues. Ann. N. Y. Acad. Sci. 591 (1), 109–127. https://doi.org/10.1111/j.1749-6632.1990.tb15084.x.

Mandal, Saptarshi, El-Amin, Ammaarah, Alexander, Kaitlyn, Rajendran, Bipin, Jha, Rashmi, 2014. Novel synaptic memory device for neuromorphic computing. Sci. Rep. 4 https://doi.org/10.1038/srep05333.

Mayergoyz, I.D., 2003. Mathematical models of hysteresis and their applications. Mathematical Models of Hysteresis and Their Applications. https://doi.org/10.1016/B978-0-12-480873-7.X5000-2.

Menon, Vinod, Uddin, Lucina Q., 2010. Saliency, switchin, attention and control: a network model of insula function. Brain Struct. Funct. 214 (5–6), 655–667. https://doi.org/10.1007/s00429-010-0262-0.Saliency.

Movshon, Adelson, Gizzi, Newsome, Movshon, J a, Adelson, Edward H., Gizzi, M.S., Newsome, W.T., 1985. The analysis of moving visual patterns. Pattern Recognition Mech 54 (13), 117–151. https://doi.org/10.1098/rstb.1998.0333.

Oldfield, R.C., 1971. The assessment and analysis of handedness: the edinburgh inventory. Neuropsychologia 9 (1), 97–113. https://doi.org/10.1016/0028-3932(71)90067-4.

Pearson, Joel, Brascamp, Jan, 2008. Sensory memory for ambiguous vision. Trends Cognit. Sci. 12 (9), 334–341. https://doi.org/10.1016/j.tics.2008.05.006.

Pelli, D.G., 1997. The VideoToolbox software for visual Psychophysics: transforming numbers into movies. Spatial Vis. 10 (4), 437–442. https://doi.org/10.1163/156856897X00366.

Pisarchik, Alexander N., Jaimes-Reátegui, Rider, Magallón-García, C. D Alejandro, Castillo-Morales, C. Obed, 2014. Critical slowing down and noise-induced intermittency in bistable perception: bifurcation analysis. Biol. Cybern. 108 (4), 397–404. https://doi.org/10.1007/s00422-014-0607-5.

Rebola, José, Castelhano, João, Ferreira, Carlos, Castelo-Branco, Miguel, 2012. Functional parcellation of the operculo-insular cortex in perceptual decision making: an FMRI study. Neuropsychologia 50 (14), 3693–3701. https://doi.org/10.1016/j.neuropsychologia.2012.06.020.

Sacharin, Vera, Sander, David, Scherer, Klaus R., 2012. The perception of changing emotion expressions. Cognition and Emotion. https://doi.org/10.1080/02699931.2012.656583.

Satterthwaite, Theodore D., Elliott, Mark A., Gerraty, Raphael T., Ruparel, Kosha, James, Loughead, Calkins, Monica E., Eickhoff, Simon B., et al., 2013. An improved framework for confound regression and filtering for control of motion artifact in the preprocessing of resting-state functional connectivity data. Neuroimage 64 (1), 240–256. https://doi.org/10.1016/j.neuroimage.2012.08.052.

Schwiedrzik, Caspar M., Ruff, Christian C., Lazar, Andreea, Leitner, Frauke C., Singer, Wolf, Melloni, Lucia, 2014. Untangling perceptual memory: hysteresis and adaptation map into separate cortical networks. Cerebr. Cortex 24 (5), 1152–1164. https://doi.org/10.1093/cercor/bhs396.

Sheremata, S.L., Bettencourt, K.C., Somers, D.C., 2010. Hemispheric asymmetry in visuotopic posterior parietal cortex emerges with visual short-term memory load. J. Neurosci. https://doi.org/10.1523/JNEUROSCI.2689-10.2010.

Sheremata, S.L., Silver, M.A., 2015. Hemisphere-dependent attentional modulation of human parietal visual field representations. J. Neurosci. https://doi.org/10.1523/JNEUROSCI.2378-14.2015.

Sousa, Teresa, Sayal, Alexandre, Duarte, João V., Costa, Gabriel N., Martins, Ricardo, Castelo-Branco, Miguel, 2018. Evidence for distinct levels of neural adaptation to both coherent and incoherently moving visual surfaces in visual area hMT+. Neuroimage 179, 540–547. https://doi.org/10.1016/j.neuroimage.2018.06.075.

Sterzer, Philipp, Kleinschmidt, Andreas, 2010. Anterior insula activations in perceptual paradigms: often observed but barely understood. Brain Struct. Funct. 214 (5–6), 611–622. https://doi.org/10.1007/s00429-010-0252-2.

Sterzer, Philipp, Kleinschmidt, Andreas, Rees, Geraint, 2009. The neural bases of multistable perception. Trends Cognit. Sci. https://doi.org/10.1016/j.tics.2009.04.006.

Sterzer, Philipp, Rees, Geraint, 2008. A neural basis for percept stabilization in binocular rivalry. J. Cognit. Neurosci. 20 (3), 389–399. https://doi.org/10.1162/jocn.2008.20039.

Talairach, J., Tournoux, P., 1988. Co-Planar Stereotaxic Atlas of the Human Brain: 3-D Proportional System: an Approach to Cerebral Imaging. Thieme Medical Publisher, New York, NY.

Torre, Maria Susana, Masoller, Cristina, 2010. Dynamical hysteresis and thermal effects in vertical-cavity surface-emitting lasers. IEEE J. Quant. Electron. 46 (12), 1788–1794. https://doi.org/10.1109/JQE.2010.2046139.

Uddin, L., 2015. Salience processing and insular cortical function and dysfunction. Nat Rev Neurosci 16, 55–61. https://doi.org/10.1038/nrn3857.

Wallach, H., 1935. Über visuell wahrgenommene bewegungsrichtung. Psychol. Forsch. 20, 325–380. https://doi.org/10.1007/BF02409790.

Wang, M., Arteaga, D., He, B.J., 2013. Brain mechanisms for simple perception and bistable perception. In: Proceedings of the National Academy of Sciences. https://doi.org/10.1073/pnas.1221945110.

Williams, Douglas, Phillips, Gregory, Sekuler, Robert, 1986. Hysteresis in the perception of motion direction as evidence for neural cooperativity. Nature 324 (6094), 253–255. https://doi.org/10.1038/324253a0.

Wilson, Hugh R., 2017. Binocular contrast, stereopsis, and rivalry: toward a dynamical synthesis. Vis. Res. 140, 89–95. https://doi.org/10.1016/j.visres.2017.07.016.

Wilson, Hugh R., 1977. Hysteresis in binocular grating perception: contrast effects. Vis. Res. 17 (7), 843–851. https://doi.org/10.1016/0042-6989(77)90128-6.

Wilson, Hugh R., 2007. Minimal physiological conditions for binocular rivalry and rivalry memory. Vis. Res. 47 (21), 2741–2750. https://doi.org/10.1016/j.visres.2007.07.007.

Wuerger, Sophie, Shapley, Robert, Rubin, Nava, 1996. "On the visually perceived direction of motion" by Hans Wallach: 60 Years later. Perception 25 (11), 1317–1367. https://doi.org/10.1068/p251317.

Zaniboni, Massimiliano, 2018. Short-term action potential memory and electrical restitution: a cellular computational study on the stability of cardiac repolarization under dynamic pacing. PloS One 13 (3). https://doi.org/10.1371/journal.pone.0193416.

Zhang, Yang, Zhou, Wenjing, Wang, Siyu, Zhou, Qin, Wang, Haixiang, Zhang, Bingqing, Huang, Juan, Hong, Bo, Wang, Xiaoqin, 2018. The roles of subdivisions of human insula in emotion perception and auditory processing. Cerebral Cortex 1–12. https://doi.org/10.1093/cercor/bhx334.